Chapter 8

# Glass Patterning: Technologies and Applications

Nguyen Van Toan, Naoki Inomata,
Masaya Toda and Takahito Ono

Additional information is available at the end of the chapter

http://dx.doi.org/10.5772/intechopen.74179

**Abstract**

In this work, we review the progress in recent studies on glass patterning including technologies and applications. Four technologies for glass micromachining including wet etching, sandblasting, reactive ion etching, and glass reflow process are analyzed. Advantages as well as disadvantages of each method are presented and discussed in light of the experiments. Various microsystem applications using the above glass patterning technologies like thermal sensors, hermetically packaged capacitive silicon resonators, optical modulator devices, glass microfluidics, micro-heaters, and vacuum-sealed capacitive micromachined ultrasonic transducer arrays are reported.

**Keywords:** wet etching, sandblasting, dry etching, glass reflow process, thermal sensors, capacitive silicon resonators, microfluidic, micro-heater, capacitive micromachined ultrasonic transducer

## 1. Introduction

Nowadays, micro/nano systems play a vital role in innovation in all areas of our life. They are utilized in almost all electrical equipments including cameras, televisions, smartphones, laptop computers, and vehicles, not only to increase the functionality but also to enhance the performance in various operating conditions. Their market is currently dominated by radio frequency (RF) microelectromechanical systems (MEMS), microfluidics, optical MEMS, gyroscopes, accelerometers, microphones, pressure sensors, and inkjet heads. Thus, micro/nano systems are being a mainstream for the electrical equipment.

Silicon and glass are the most commonly used materials in microsystems, employed for the fabrication of a wide range of microdevices [1–5]. Patterning of silicon structures, which has

been studied and developed for years, can be done by both wet (KOH and tetramethyl ammonium hydroxide (TMAH)) [6] and dry (reactive ion etching) etching methods. Forming high aspect ratio silicon structures could be easily achieved by deep RIE (Bosch process) technique [7]. In turn, glass micromachining faces difficulties owing to its components. Tempax glass is one kind of borosilicate glass which is frequently used in the microfabrication owing to low cost, good thermal insulation, excellent optical transparency, and anodic bonding capability. Tempax glass [5] is approximately composed of 75% $SiO_2$, 13% $Na_2O$, 10.5% CaO, and other minor additives such as 1.3% $Al_2O_3$, 0.3% $K_2O$, etc. Different compositions exhibit a different rate in the etching process so that low aspect ratio structure, etching rate, and mask selectivity are still current issues in glass micromachining. Tempax glass exhibits the excellent mechanical (mechanical strength and stiffness), dielectric (high electric insulation), and optical (high transparency) properties. In addition, it is a bio-compatible material [8]. The thermal expansion coefficient of glass is similar to that of silicon this allowing to produce silicon-on-glass substrates via an anodic bonding technique [4]. High electric insulation becomes a significant point to reduce the signal loss (parasitic capacitances) in RF MEMS, especially in high-frequency ranges and nanomechanical resonant structures [9].

In this work, we review the recent progress in glass micromachining and its applications for the microsystem fabrications. The various glass patterning technologies including wet etching, sandblasting, the reactive ion etching, and glass reflow process are presented together with the microsystem applications including thermal sensors, hermetically packaged capacitive silicon resonators, optical modulator devices, glass microfluidics, micro-heaters, and vacuum-sealed capacitive micromachined ultrasonic transducer (CMUT) arrays.

## 2. Wet etching and sandblasting

### 2.1. Description

The wet etching of glass reported in the literature [10, 11] is one of the simple methods for glass patterning; nevertheless, the precisely formed glass structure is difficult owing to its isotropic etching behavior. Advantages and disadvantages of the wet etching method are compared to other methods including sandblasting, RIE, and glass reflow process as shown in **Table 1**. High mask selectivity, low surface roughness, and simple operation are advantages of the wet etching. In turn, wet etching method cannot be used for forming small glass structures, below 1 μm-diameter. Also, created glass structures face a problem of the aspect ratio. Aspect ratio structure of glass patterning via this method is just below 1.

**Figure 1** illustrates the wet etching process of glass which begins with a glass substrate of 300-μm-thick (**Figure 1(a)**). Both sides of the glass substrate are coated with 30-nm-thick Cr and 300-nm-thick Au layers (**Figure 1(b)**). Cr-Au layers increase the adhesion of the glass substrate and photoresist. Cr has a good adhesion with glass substrate while Au is an inert material in the diluted HF solution. Next, a photoresist is deposited and patterned by a photolithography process. The back side of the glass substrate is also coated with the photoresist. The Cr-Au layer is then etched out by the wet etchant, as shown in **Figure 1(c)**. Finally, the

| Parameters | Wet etching | Sandblasting | RIE | Glass reflow |
|---|---|---|---|---|
| Feature size | | | | |
| Minimum size | 1 μm | 100 μm | <1 μm | <1 μm |
| Side etching | Yes | No | No | No |
| Etching profile | U shapes | V shapes | Vertical | Vertical |
| Aspect ratio | Low | Low | High | High |
| Surfaces | Smooth | Rough | Smooth | Smooth |
| Process time | Short | Short | Medium | Long |
| Mask materials | Metal and photoresist | Dry film resist | Metal mask for high selectivity | Silicon mold |
| Selectivity between Tempax glass and mask material | High | Low | High | Glass fills into cavity |
| Etching environment | Liquid | $Al_2O_3$ particles | Plasma | Atmospheric furnace with a high temperature |
| Post processes | Good | Particles | Good | Good |

**Table 1.** Summarized advantages and disadvantages of glass micromachining.

wafer is dipped in the diluted HF (**Figure 1(d)**). The wet etching setup is shown in **Figure 1(f)**. The etching rate is a function of the concentration of the diluted HF. Higher etching rate can be achieved by increasing the concentration of the diluted HF; nevertheless, the quality of the photoresist mask becomes poor. In this demonstration, the Tempax glass was etched using the diluted solution of 50% HF:DI (deionized water) = 2:1 for etching time of 10 min. Etching rate and side etching were observed at around 2 μm/min. **Figure 2(a)** and **(b)** show the experimental results of Cr-Au wet etching and glass etching, respectively.

For short patterning glass structures, the wet etching is the preferred way; however, the large depth patterning glass structures face difficulties owing to the high etching rate of the side etching. In order to solve this issue, sandblasting is considered. This is the physical etching method where a particles jet is directed toward a sample (glass substrate) for mechanical erosion via the impingement of high-velocity abrasive particles. Not only glass but also other materials including ceramic and silicon can also be patterned via this method.

**Figure 3** describes the sandblasting process which uses thick dry film resist (MS 7050, 50 μm thickness, Mitsubishi paper mills limited., Japan) as a mask material. 300-μm-thick glass substrate is used (**Figure 3(a)**). A dry film resist is pasted, and then photolithography is performed, as shown in **Figure 3(b)**. Next, the glass substrate with a dry film resist patterns is etched via sandblast. **Figure 4** shows a glass patterning with an etching depth of approximately 150 μm. Glass etching surfaces are very rough and etching profiles evolve into V-shapes. Etching through the glass substrate is possible and generally it is employed for microfluidics which need holes for an inlet and outlet of liquid.

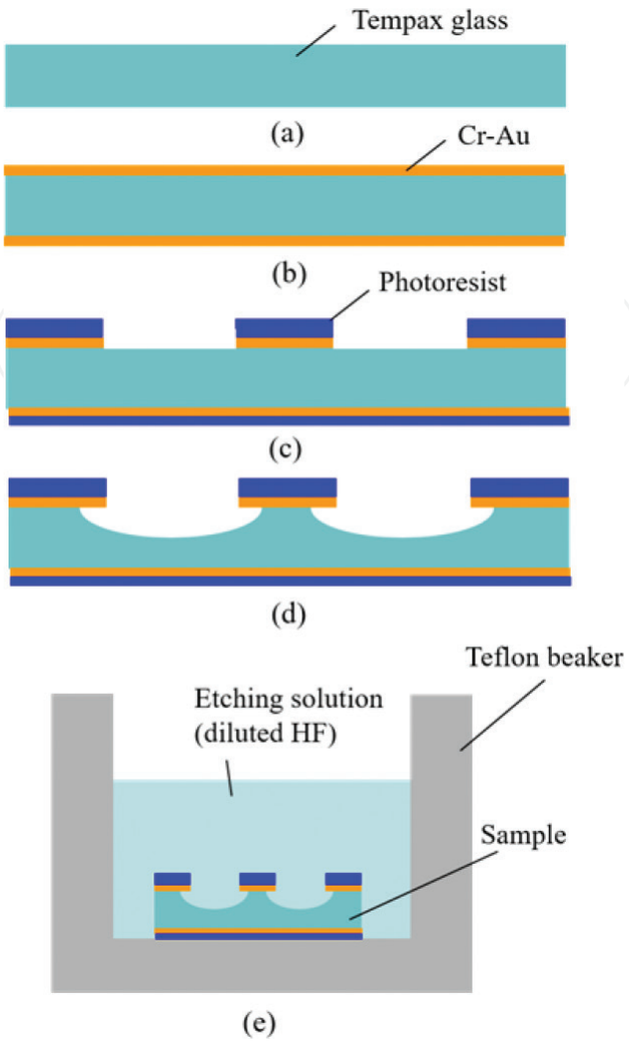


**Figure 1.** Wet etching process. (a) Tempax glass. (b) Cr-Au sputter. (c) Photolithography and Cr-Au wet etching. (d) Glass wet etching. (e) Wet etching setup.

## 2.2. Typical applications using wet etching and sandblasting

Generally, wet etching and sandblasting methods are employed for the glass patterning without requiring highly precise structure including large channels for microfluidics, through holes for inlet and outlet liquid in microfluidic, and cavities for microfabricated resonators, as described in the following.

### *2.2.1. Thermal sensors for heat detection of living cells in liquid*

Heat of cells generated by biochemical reactions is one of the critical parameters of living organisms. Monitoring heat of cells is an effective way of investigating cell activities; however, heat production is associated with very small values. It means that the heat losses become a serious problem for heat detection. Low thermal conductivity of glass is one of the good characteristics that make it popular in thermal sensors [12–14]. In this section, we propose and developed heat-detecting silicon resonators which rely on temperature-dependent changes in the resonant frequency of resonators.

http://dx.doi.org/10.5772/intechopen.74179

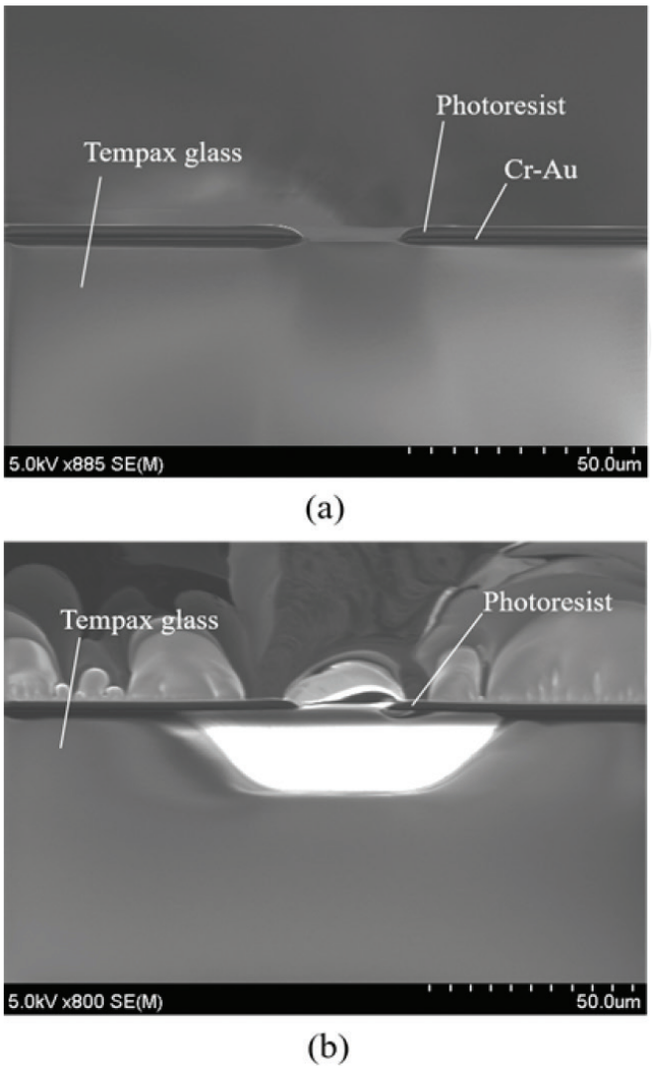


**Figure 2.** (a) Photolithography and metal etching. (b) Glass etching result.

**Figure 5(a)** shows the proposed resonant thermal sensor for heat detection of a living cell in a liquid which consists of a glass microfluidic, silicon cantilever, and vacuum chamber. The vacuum chamber and microfluidic are separated by a glass wall. Silicon cantilever is employed as a heat guide from the microfluidic to the vacuum chamber. The heat generated by a cell attached to the silicon cantilever in the microfluidic side is conducted to the silicon resonator in vacuum chamber side and the resulting temperature changes cause a shift in the resonant frequency of the silicon cantilever.

The thermal sensor is fabricated by well-known technologies including photolithography, wet etching, and anodic bonding. Vacuum chamber and microfluidic are formed by the wet etching method and holes for inlet and outlet liquids are patterned by the sandblasting method. **Figure 5(b)** shows the optical image of the completely fabricated device with an attached cell in silicon cantilever in the microfluidic. The details of the experimental processes and evaluation for this device can be found in [12].

In summary, microfluidics, vacuum chambers, and through holes of the glass substrate are successfully patterned by the wet etching and sandblasting methods. The use of resonant

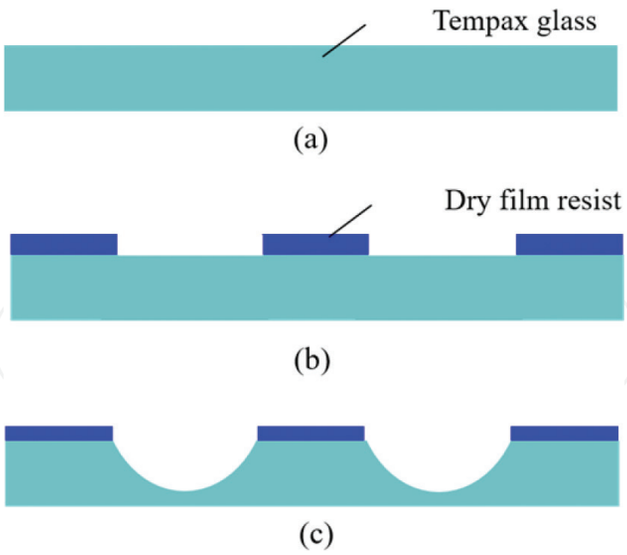


**Figure 3.** Fabrication process. (a) Tempax glass (b) Photolithography with a dry film resist. (c) Sandblasting.

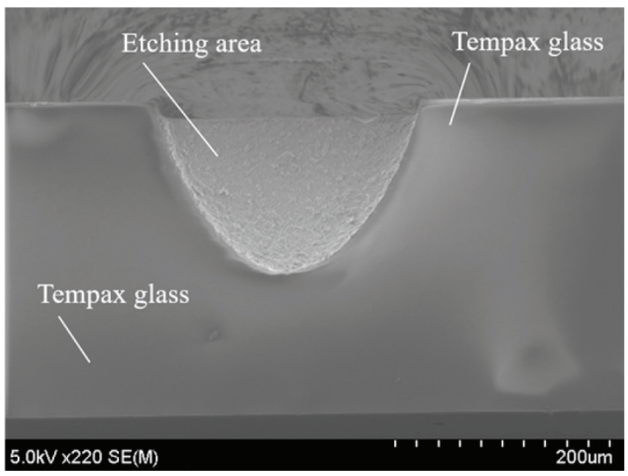


**Figure 4.** Glass cavity by sandblasting.

thermal sensors to measure the generated heat of a biological cell in a liquid is a clear example. The proposed devices are promising for biochemical reaction monitoring.

*2.2.2. Hermetically packaged capacitive silicon resonators*

Thermal expansion coefficient of glass is similar to that of silicon which makes them easily bonded together via an anodic bonding method [15]. Silicon-glass bonding becomes a key technology for device integration in various fields including microelectromechanical systems (MEMS), microelectronics, and optoelectronics. Anodic bonding between the glass substrate and silicon was employed in our works including the parasitic capacitance reduction [9, 16] and hermetically packaged device [4]. The structures of the resonator on silicon-on-insulator

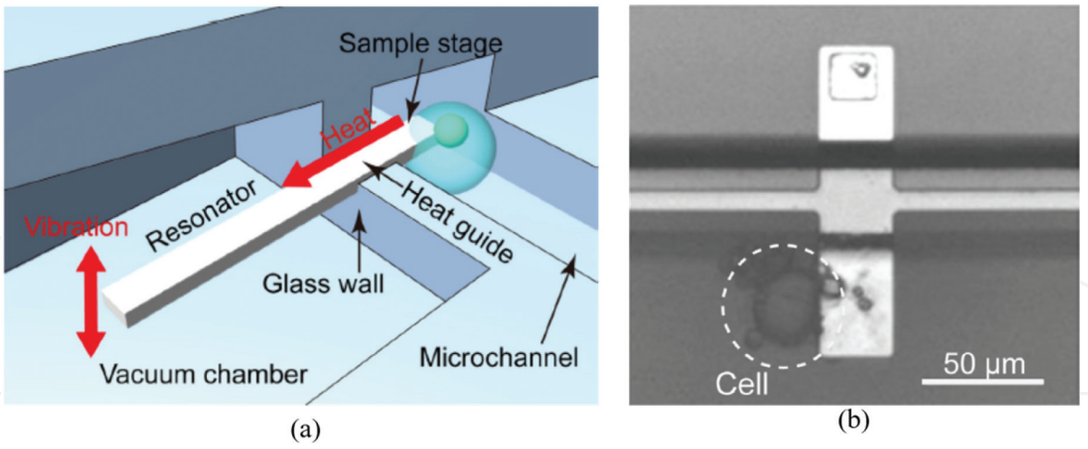


**Figure 5.** (a) Resonant thermal sensor for heat detection of living cells in liquid. (b) Fabricated device with an attached cell.

(SOI) are transferred to the glass substrate in order to reduce the parasitic capacitances from the handling silicon layer, as presented in [9]. Here, we present the hermetically packaged capacitive silicon resonator based on the anodic bonding.

Capacitive silicon resonators, typically employed for sensing applications and timing references, have been presented in many works [3, 4]. Their output signal is based on the measurement of the change in the capacitance between a sensing electrode and the resonant body. **Figure 6(a)** shows the sketched cross-section image of our proposed capacitive silicon resonator where the resonant bodies are placed between driving/sensing electrodes, supported by two thin beams on the sides and separated by the narrow capacitive gaps (**Figure 6(b)**). The capacitive resonator's operation is described as follows: when an AC voltage $V_{AC}$ is applied to the driving electrode, the resulting electrostatic force induces a bulk acoustic wave in the resonant element. An additional DC voltage $V_{DC}$ is also applied to the driving/sensing electrodes in order to amplify the electrostatic force. Small changes in the size of the sensing gap generate a voltage on the sensing electrode.

The structures of silicon resonator are defined by the deep RIE on SOI wafer and then transferred on to LTCC (low temperature co-fired ceramic) substrate with metal feed-through for electrically connected to silicon electrodes. The device is hermetically packaged by the anodic bonding technique between silicon and glass. **Figure 6(b)** and **(c)** show the optical images of the silicon resonator structure on LTCC substrate and the 2×2 $cm^2$ glass substrate with patterning obtained by the sandblasting for the packaging step. Front and back sides of the fabricated device after packaged process are shown in **Figure 6(d)** and **(e)**, respectively. The details of the fabrication process and evaluation of the proposal device can be found in [4].

In summary, the glass can be used as a material for the hermetically packaged. Glass and silicon can be well bonded together via the anodic bonding technique. The hermetically packaged capacitive silicon resonators were successfully demonstrated.

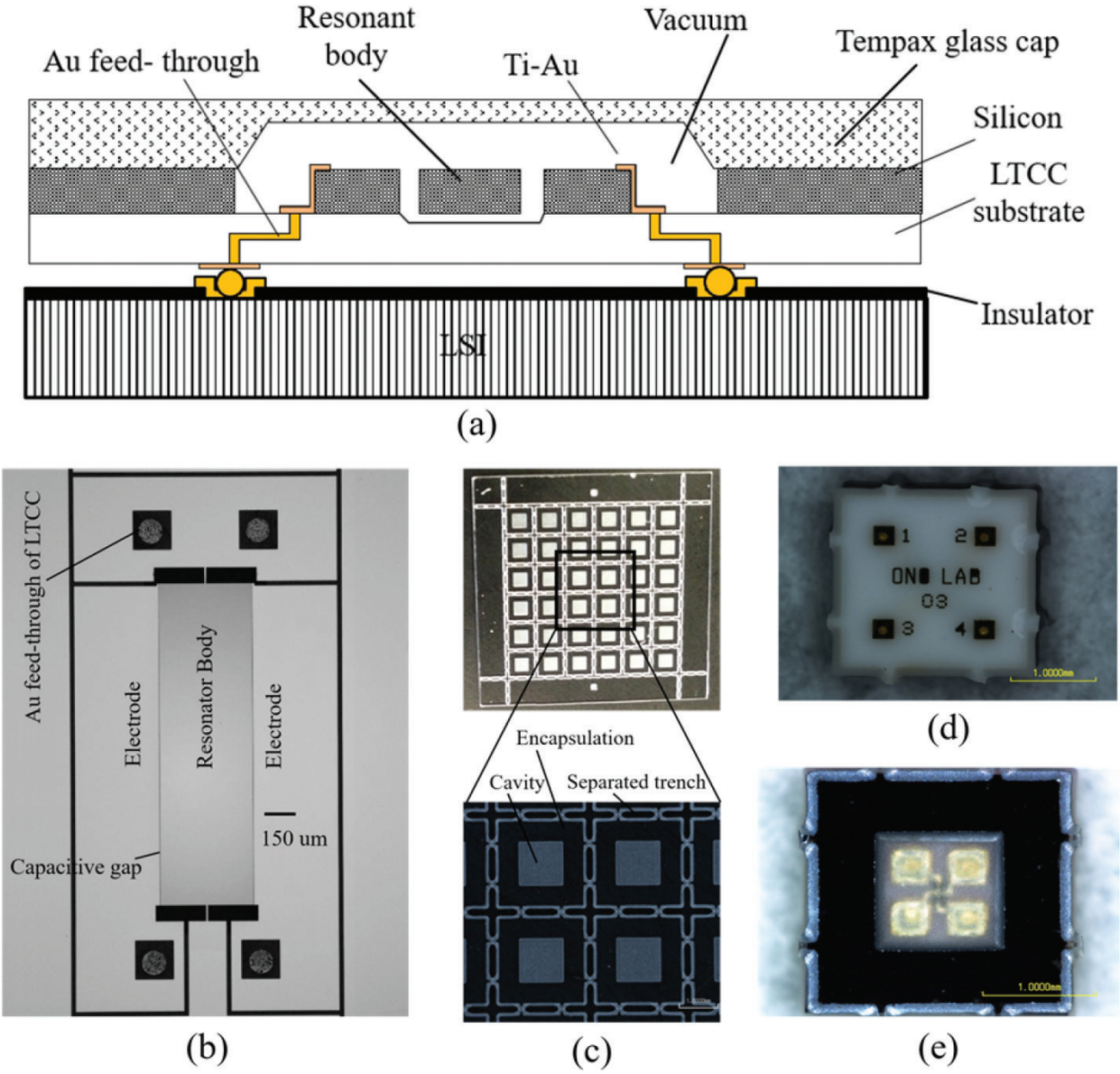


**Figure 6.** (a) Cross-section of the hermetically packaged silicon capacitive resonator. (b) Micrograph of silicon resonator on LTCC substrate. (c) 2×2 cm glass substrate with sandblasting patterning. (d) Front and (e) back sides of the device after hermetically packaged.

## 3. Reactive ion etching

### 3.1. Description

Although wet etching and sandblasting methods for glass patterning are widely used for microsystems, they face problems including small pattern structures and dimension reproducibility. In this section, we present the RIE method which can be potentially used for accurately patterning small glass structures.

**Figure 7** shows our laboratory-made RIE equipment for the deep glass etching which is a kind of magnetron-type RIE. A strong permanent magnet (samarium-cobalt (Sm-Co)) is placed

on the top glass cover to enhance plasma density. A small etching chamber with an internal diameter of 145 mm is employed. The distance between the top glass cover and the sample stage is 13 mm. The chamber is evacuated by a turbo-molecular pump with a pumping speed of 300 l/s during the etching process which helps to reduce the deposition of reaction products on the sample surface. Plasma is generated by a 13.56 MHz RF generator and connected to the cathode. The cathode is made by aluminum with 80 mm diameter and isolated from a grounded circular cooling system by a Teflon for stray capacitance reduction. Samples are attached to the cathode stage using silicone grease for heat conduction to the stage.

**Figure 8** describes the sample preparation process for the deep etching glass. It starts with a 300 μm-thick Tempax glass substrate (**Figure 8(a)**). After simple cleaning procedures (acetone, ethanol, and piranha), the glass substrate is sputtered by Cr-Au thin films with a thickness of 10 and 40 nm, respectively, as a seed layer for an electroplating of Ni (**Figure 8(b)**). A 600 nm-thick Ni film is formed on the Cr-Au surface with photoresist patterning (**Figure 8(c)** and **(d)**). Finally, the glass substrate is etched out by the above RIE setup mentioned.

The RIE etching result of the above-mentioned process is shown in **Figure 9**. Deep glass pillars with a smooth surface, vertical shapes (base angle ~ 89°) and high aspect ratio (=10) with depth of 10 μm, diameter of 1 μm and pitch of two pillars of 2 μm were achieved. The details of etching conditions and effects of the mask shape profiles can be found in [17].

### 3.2. Typical applications using reactive ion etching

#### *3.2.1. Optical modulator*

High transparency characteristic of glass was employed for many optical systems based on micro-optical-electro-mechanical-systems, as previously reported [17–19]. Optical devices allow manipulation of light including amplitude [20] and phase [21]. In this section, we show an optical modulator device capable of the integration of an image sensor for functional image sensing applications.

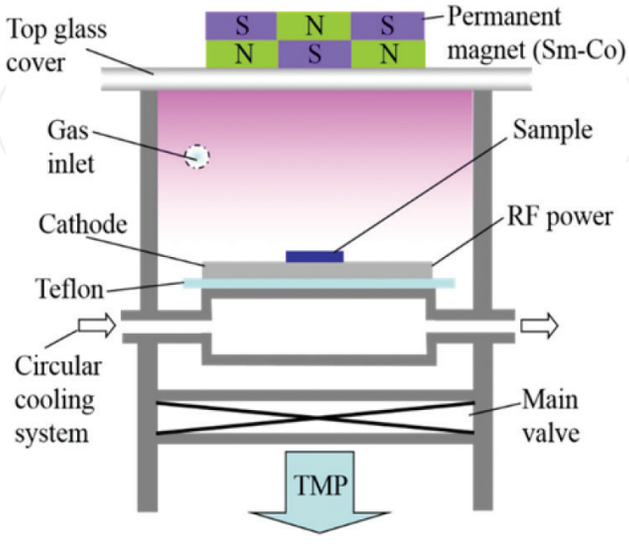


**Figure 7.** Reactive ion etching setup.

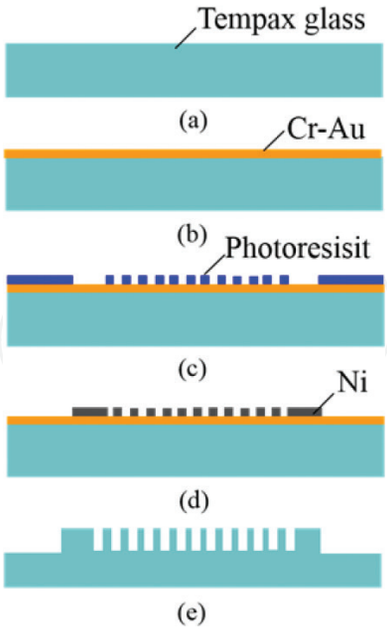


**Figure 8.** Glass patterning by RIE. (a) Tempax glass wafer. (b) Cr-Au sputter. (c) Photolithography. (d) Nickel electroplating and photoresist removal. (e) RIE process.

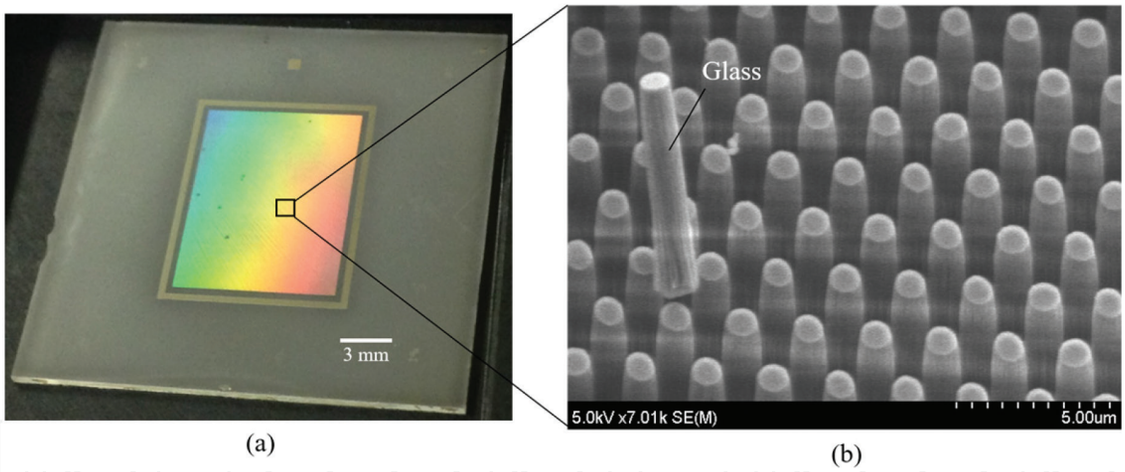


**Figure 9.** Glass pillar by RIE. (a) Optical image of 2×2 cm glass wafer with pillar patterning at center (colorful area). (b) Close-up scanning electron microscope (SEM) image of the pillar patterning area.

The device structure is illustrated in **Figure 10**. The 7.2×9.6 mm optical window area consists of glass pillar structures assembled with a liquid reservoir. The electrode material of top and bottom electrodes is aluminum-doped zinc oxide (AZO) produced by atomic layer deposition (ALD) method. This device can be directly mounted on an image sensor chip and has a large optical modulation range.

The optical window is operated using a dynamic electrical control of the wetting behavior of liquid on the top of the micropillar surfaces. Device concept was reported in [19, 22, 23]. When a voltage is applied to the structure, the liquid moves into the spaces between the pillars (**Figure 10(b)**). The light reflection at the pillar sidewalls is eliminated because of the

refractive index matching at the interface; therefore, the pillars array gets transparent. Thus, a high optical transmittance is obtained. In the case without liquid between pillars, the light transmittance of the device is lower than that with liquid because of light reflection and scattering by pillar walls and it works ideally as an opaque medium (**Figure 10(a)**). Therefore, by shifting the liquid in and out of the pillar array using electro-wetting, the light transmittance can be electrically controlled.

Glass pillar structures are produced by RIE, as reported before (**Figure 9**). **Figure 10(c)** shows the optical evaluation setup. It contains a cold-cathode fluorescent lamp for illumination, a resolution chart for the optical property evaluation, a focal length and F-number of the camera lens, and an image sensor. A matching oil is inserted into the pillars array just by putting the liquid droplet on the device that immediately penetrates in the whole area of the optical window. **Figure 10(d)** shows a comparison of transmittance with and without liquid penetration by using an image sensor. A low transmittance of the optical window is observed when it is measured without inserting the matching oil for glass pillar structures. The low transmission light, in this case, causes light reflection and scattering by pillar walls. A very high transmitting light of around 90% can be achieved by using matching oil. The possible reason is due to the refractive index matching between glass pillars and matching oil. Thus, the large modulation range of approximately 65% for cases with and without matching oil is achieved.

In summary, glass is a potential material for optical systems owing to its highly transparent property. The optical device based on glass patterning by RIE with the large optical modulation range was demonstrated. This device can be directly mounted on an image sensor chip for functional image sensing applications.

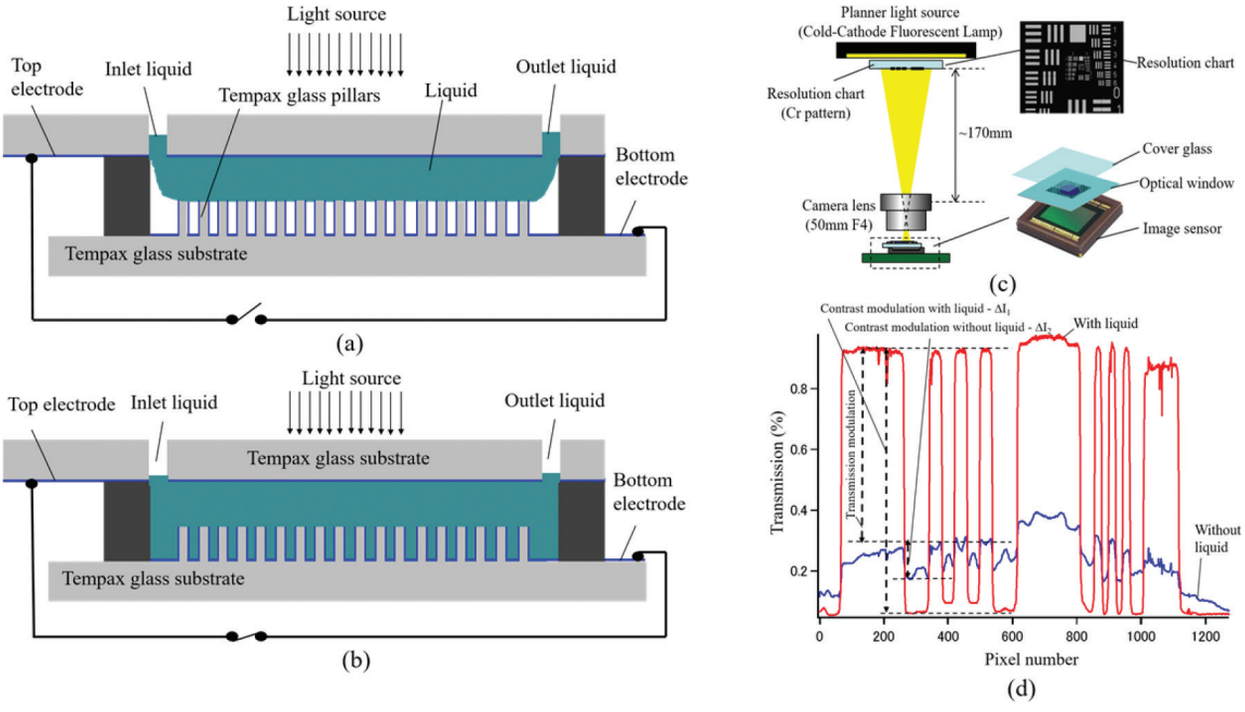


**Figure 10.** (a) Opaque state (without voltage supply). (b) Transparent state (with voltage supply). (c) Evaluation setup. (d) Optical property evaluation of optical window with and without liquid penetration.

*3.2.2. Glass microfluidic integrated with thin silicon layer for observation of biological samples*

Microfluidics has huge potential for bio-applications [12–14]. The bio-compatible selection of microfluidic material is important to avoid any effects on biological samples. Thus, a glass material becomes the preferred one for bio-applications [8]. Also, high-resolution observation of living cells helps more understanding of biological functions through the study of cellular dynamics. The surface structure of cancer cells was observed in nanoscale using scanning electron microscopy (SEM) and transmission electron microscopy (TEM), as reported in [24]. A floating particle in the liquid was observed with a TEM system using the microfluidic chamber [25]. In this section, the glass microfluidics integrated with a thin window of silicon layer for the observation of biological samples using a SEM system is described.

**Figure 11(a)** shows the proposed structure consisting of micro-channels (trapping channel and bypass channel), a thin silicon layer on top of the channels, a trapping pole, an inlet, and an outlet of liquid sample. At first, micro-channels are patterned by reactive ion etching (RIE) with nickel metal as a mask material. Then, SOI wafer with 200 nm-thick device layer is bonded to the patterned glass surface above by anodic bonding method. The handling layer of SOI is partially etched out by deep RIE until reaching the opened insulator layer ($SiO_2$) at the window part. Finally, $SiO_2$ is removed by HF vapors.

**Figure 11(b)** shows a SEM image of the fabricated device which installed into SEM chamber. DI water is then flowed into microfluidic under SEM observation, as demonstrated in **Figure 11(c)**. The details of the fabrication process, evaluation setup, and measurement results can be found in [26].

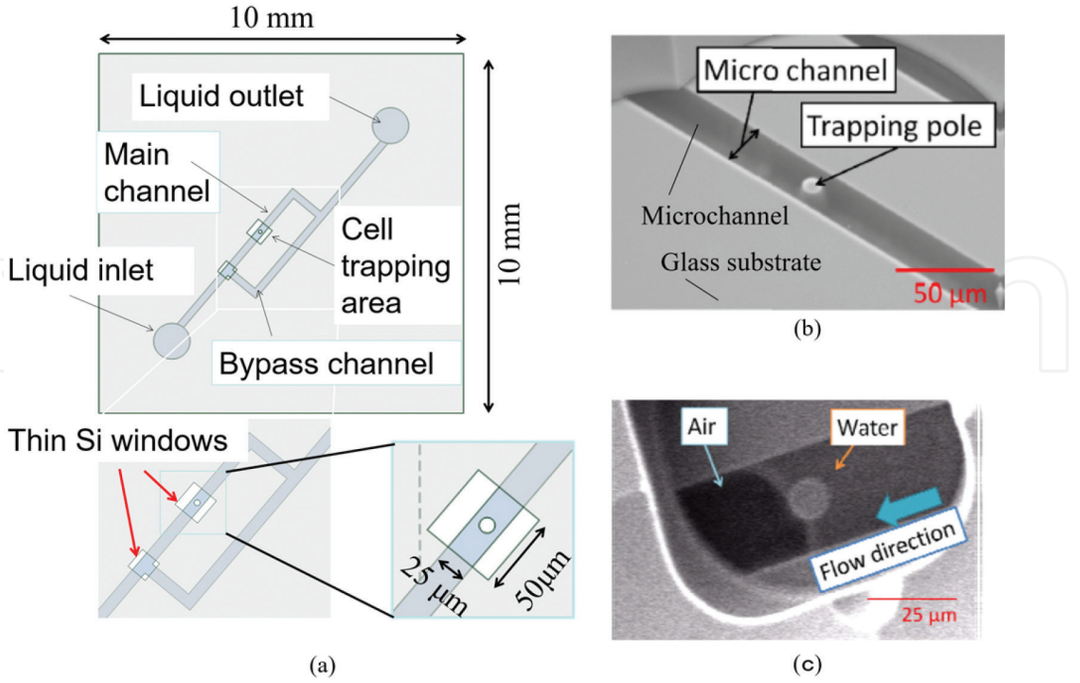


**Figure 11.** (a) Glass microfluidics integrated with a thin silicon layer for cell observation. (b) Fabricated device. (c) DI water loaded into the microfluidic under SEM observation.

In summary, glass microfluidics, successfully patterned by RIE, integrated with a thin window of silicon layer for the observation of biological samples in vacuum analytical system (ex. SEM) was demonstrated.

## 4. Glass reflow process

### 4.1. Description

Precise glass patterning can be achieved by RIE method; however, forming very deep glass structures is a challenge owing to a low etching rate and low selectivity (between the glass and mask material). Also, the reflection of ions [17] at the mask or the edge of the mask and/or mask erosion may contribute to its limited aspect ratio and depth. To overcome the above problems, glass reflow process was investigated in [18, 19] which can create the compounded structures between silicon and glass. In this section, we present glass reflow process and its applications for microsystems.

**Figure 12** schematizes glass reflow process which starts with a 300 μm-thick silicon wafer. The silicon structures (silicon mold) are formed by deep RIE based on Bosch process using $SF_6$ and $C_4F_8$ (**Figure 12(a)**). Next, anodic bonding of the silicon wafer and the Tempax glass is carried out in a high vacuum chamber with an applied voltage of 800 V at 400°C for 15 min (**Figure 12(b)**). The glass reflow process is performed in a furnace with ambient atmospheric pressure at 750°C for 10 h (**Figure 12(c)**). Tempax glass is melted and poured into cavities of silicon mold during the high-temperature glass reflow process. After that, both sides of the wafer are mechanically lapped and polished by a chemical mechanical polishing process (**Figure 12(d)**).

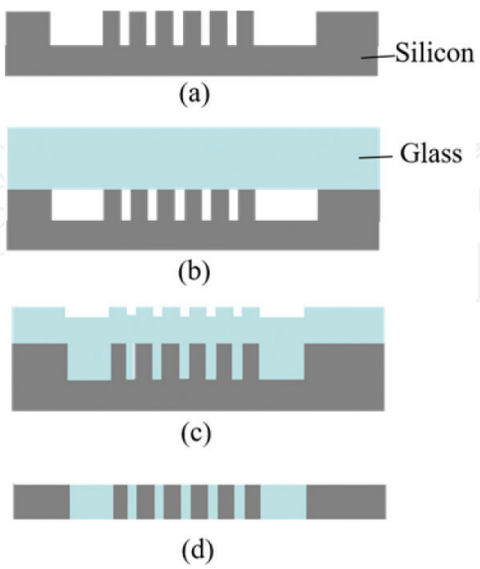


**Figure 12.** Glass reflow process. (a) Silicon mold. (b) Anodic bonding in a vacuum chamber. (c) Glass reflow process. (d) Lapping and polishing process.

**Figure 13(a)** and **(b)** show silicon mold formed by deep RIE and the compounded structure between silicon and glass created by glass reflow process, respectively. The complete filling into the cavities was achieved. Thus, the glass structures can be formed by glass reflow process; nevertheless, the process faces difficulties when glass enters into narrow patterns. Glass reflow into narrow trenches was investigated by an additional optimization of the process flow conditions. At higher temperature (1100°C) and with longer time process (20 h), using $SiO_2$ to enhance surface wettability, the complete filling glass into the narrow trenches was achieved. **Figure 14(a)** and **(b)** show the silicon pillar mold and complete filling glass into narrow trenches, respectively. The details of glass reflow process condition can be found in [18].

In summary, the glass reflow into the large cavities and narrow trenches and deep glass structures compounded with silicon can be achieved. The glass can easily fill large cavities; nevertheless, additional conditions are required for filling into the narrow trenches.

### 4.2. Typical applications using glass reflow process

The glass reflow process exhibits more advantages than wet etching, sandblasting and RIE methods. We have used it for microsystem applications, as reported in [18, 27]. We have investigated it

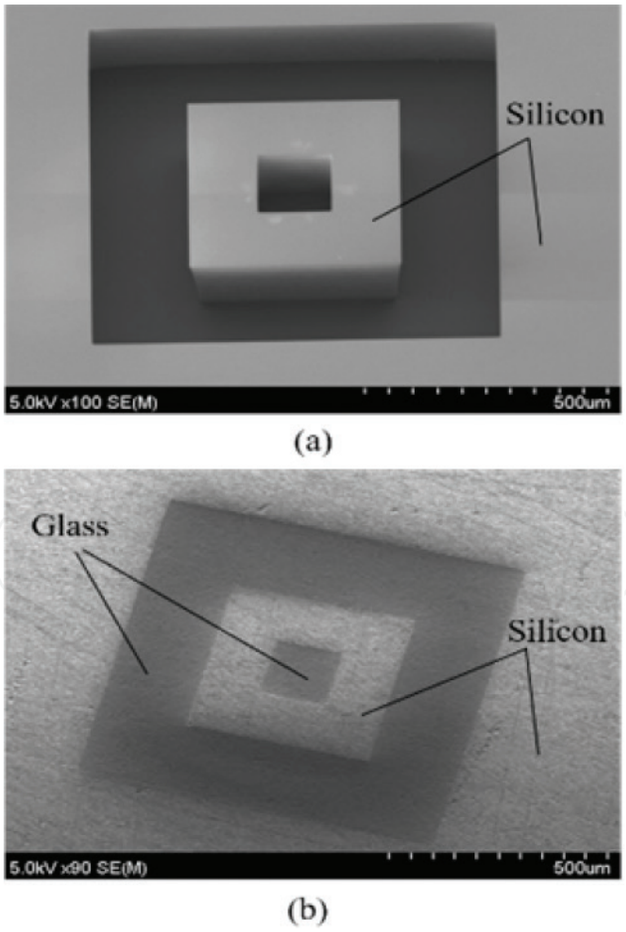


**Figure 13.** Glass reflow for large pattern size. (a) Silicon mold. (b) Glass reflow into a silicon mold.

in different of microsystems including through-wafer interconnects, thermal isolation, vacuum-sealed capacitive micromachined ultrasonic transducer (CMUT) arrays, and optical modulator devices. The optical modulator device's concept is similar to that in Section 3.2.1. The details of fabrication process and evaluation can be found in [22]. Here, we report thermal isolation and CMUTs, as follows.

*4.2.1. Thermal isolation*

Micro-heaters are typically used in the gas chemical sensors [28, 29] because the gas chemical reactions in a sensing layer require a high temperature. Micro-heaters are considered as a hot plate which controls the temperature of the sensing layer. Furthermore, they may also be used as an infrared source to analyze the molecular fingerprint of gases using infrared gas sensors [30]. Moreover, several MEMS devices require a good thermal isolation such as infrared detectors [31] and ultrasonic transducers for thermal applications [32]. Thus, the good thermal isolation is very desirable in micro/nano thermal devices. Glasses are suitable materials for this purpose because of their low thermal conductivity, low thermal expansion coefficient

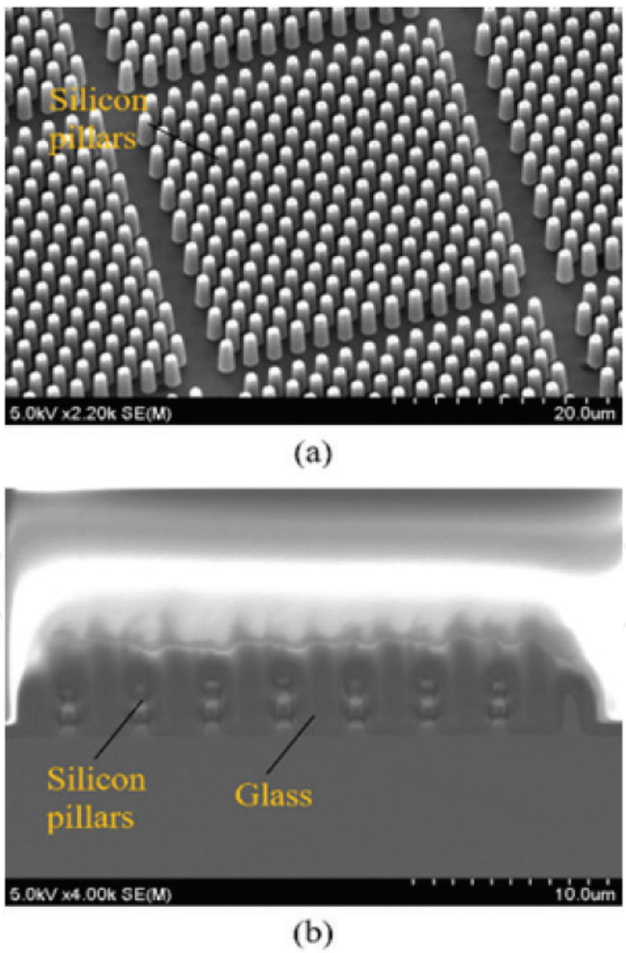


**Figure 14.** Glass reflow for small pattern size. (a) Silicon mold. (b) Glass reflow into a silicon mold.

and excellent mechanical strength. $SiO_2$ layers of 10–100 μm thickness for thermal isolation was reported in [33], where silicon pillars have formed by deep RIE technique with the high aspect ratio structure which are then oxidized to create the $SiO_2$ layer as thick as the deep RIE patterns. Nevertheless, silicon at bottom areas may be difficult to turn completely to $SiO_2$ and pores may exist inside the $SiO_2$ layer.

A thick glass layer for thermal isolation was proposed in [18]. Silicon micro-heater is compounded by the glass substrate fabricated by the glass reflow process. Top view of the micro-heater is shown in **Figure 15(a)**. The silicon micro-heater has been characterized by the near-infrared imaging as shown in **Figure 15(b)**. The temperature distribution is highly located at the silicon part. The compounded glass can thermally isolate the heated silicon effectively with a temperature difference more than 100°C when the temperature of the silicon part is heated at 140°C at an input power of 200 mW. In addition, a reliability property of the silicon micro-heater is evaluated. The electrical current is supplied to the micro-heater and kept ON state at 140°C for more 2 hours and the response is recorded, as shown in **Figure 15(c)**, which shows highly stable temperature with ±1.5°C tolerance. Thermal cycling is also performed with repetitive ON/OFF cycles for 1.5 hours. ON/OFF states with 1 min/ 1 min cycles are applied and the response is observed which shows a good stability at the heating operation as shown in **Figure 15(d)**.

In summary, the proposed micro-heater fabricated by glass reflow process shows good characteristics that allow possible application to gas chemical sensors.

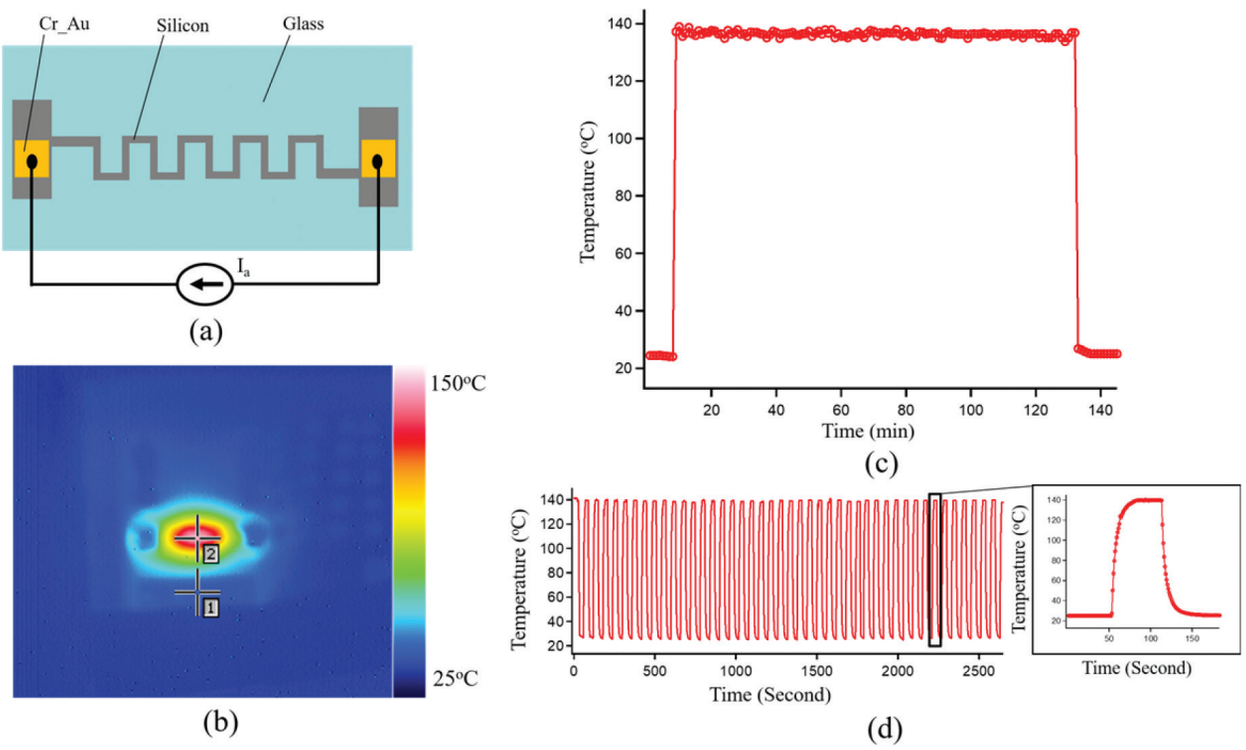


**Figure 15.** (a) Silicon micro-heater compounded glass. (b) Infracted image of silicon micro-heater. (c) Keep ON at 140°C. (d) ON/OFF cyclic test of the micro-heater.

*4.2.2. Vacuum-sealed capacitive micromachined ultrasonic transducer arrays*

CMUTs are currently present in many electrical equipment such as medical imaging, nondestructive measurement, and chemical sensing. CMUT array device produced by the glass reflow and anodic bonding reported in our recent work [27]. Firstly, we demonstrate the low resistance of the silicon through-glass wafer via based on the glass reflow process and a low resistivity silicon wafer. Secondly, the anodic bonding between silicon-glass reflow wafer and SOI wafer is successfully performed. Then, the handle and buried oxide layers are etched to release CMUT membranes and electrical connections and pads are subsequently formed via sputter method and using a shadow mask. More information on fabrication process can be found in [27].

**Figure 16(a)** shows the CMUTs structure which contains silicon through-wafer interconnects and releasing membranes suspended over vacuum gaps. The CMUT cells are separated by the Tempax glass and Cr-Au layers are employed for electrical connections and pads. The CMUT works as a capacitor cell. When a DC voltage is applied to two electrodes, the silicon

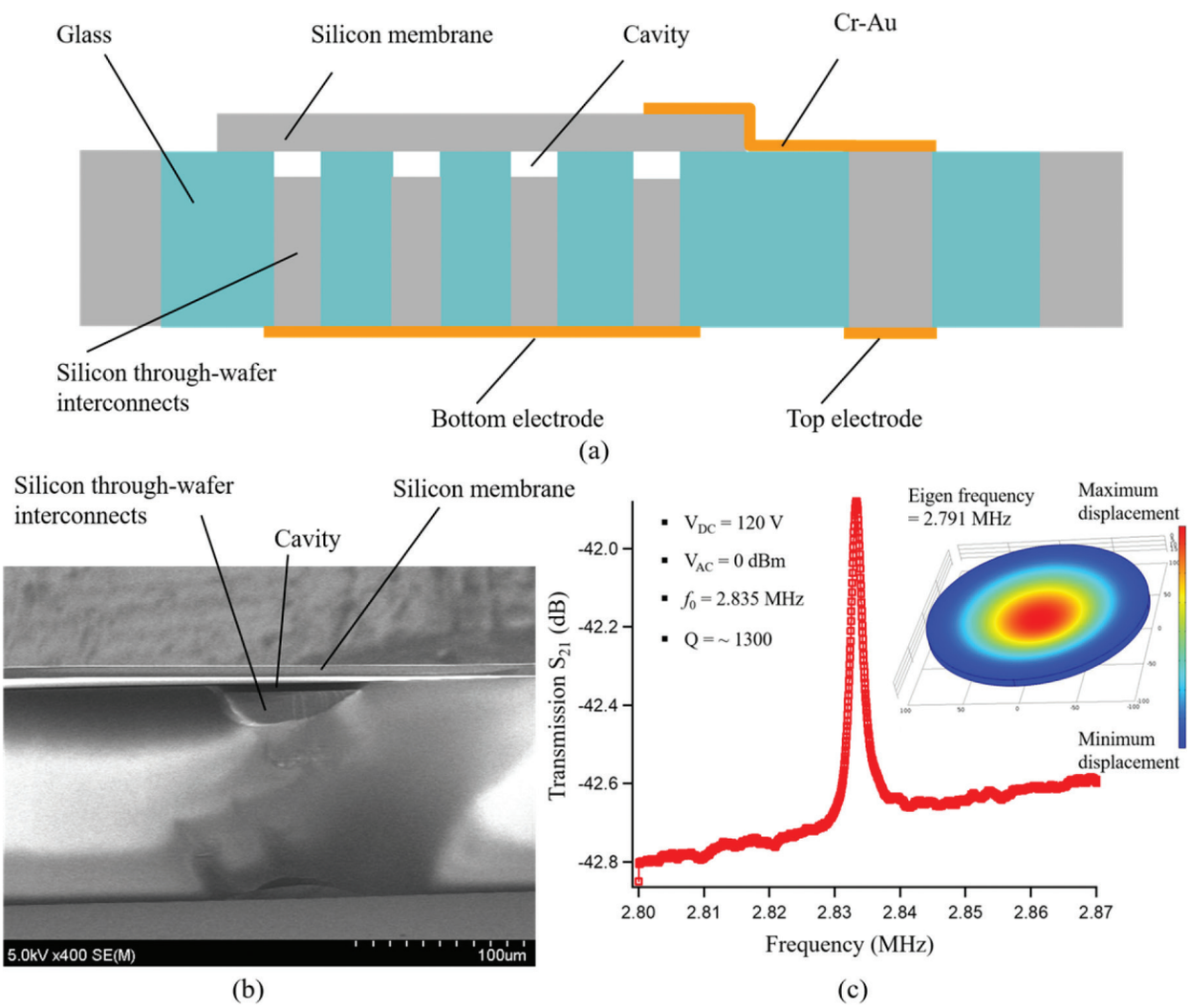


**Figure 16.** (a) Device structure. (b) Vacuum cavity. (c) Transmission $S_{21}$ of CMUTs device.

membranes are attracted toward the bottom electrode by the electrostatic force. If the AC voltage is supplied to the membrane, driving the capacitor with an alternating voltage generates ultrasound. It works as a transmitter in this case. Otherwise, if the membrane is subjected to ultrasound pressure, the electrical current is created due to the capacitance changes and in this mode, it works as a receiver.

**Figure 16(b)** shows the SEM image of a vacuum-sealed cavity. The resonance characteristic of CMUT array is evaluated using a network analyzer. Transmission $S_{21}$ is indicated for CMUT array in **Figure 16(c)**. A resonant peak, which is observed under $V_{dc}$ of 120 V, $V_{ac}$ of 0 dBm, is found at 2.83 MHz with the *Q* factor of approximately 1300 in the vacuum environment of 0.01 Pa. Additionally, the simulation result (FEM – finite element method) is in good agreement with experimental results as shown in **Figure 16(c)**.

In summary, the CMUTs device based on the glass reflow process and anodic bonding was demonstrated. The experiment process may be useful in microsystems including optical devices, microfluidics, packaging with electrical feed-through, and 3D-MEMS devices.

## 5. Conclusions

In this work, four technologies for glass micromachining including wet etching, sandblasting, RIE, and glass reflow process were reported and discussed. The wet etching and sandblasting technologies are simple process; however, they face problems including small pattern structures and dimension reproducibility. RIE technique exhibits potential for accurately patterning small glass structures, but forming very deep glass structures are a challenge owing to a low etching rate and low selectivity. Glass reflow process which creates compounded structures between silicon and glass is a suitable technology for various microsystem fabrications; nevertheless, some additional conditions are required for filling into the narrow trenches. Typical applications take advantage from the above technologies including thermal sensors, hermetically packaged capacitive silicon resonators, optical modulator devices, glass microfluidics, micro-heaters, and vacuum-sealed capacitive micromachined ultrasonic transducer arrays. It is our hope that this review may be a useful reference for those working in the field of micro/nanosystems.

## Acknowledgements

Part of this work was performed in the Micro/Nanomachining Research Education Center (MNC) of Tohoku University. This work was supported in part by JSPS KAKENHI for Young Scientists B (Grant number: 17 K14095) and also by Special Coordination Funds for Promoting Science and Technology, Formation of Innovation Center for Fusion of Advanced Technologies.

## Author details

Nguyen Van Toan*, Naoki Inomata, Masaya Toda and Takahito Ono

*Address all correspondence to: nvtoan@nme.mech.tohoku.ac.jp

Graduate School of Engineering, Tohoku University, Sendai, Japan

## References

[1] Ono T, Esashi M. Mass sensing with resonating ultra-thin silicon beams detected by a double-beam laser Doppler vibrometer. Measurement Science and Technology. 2004; **15**:1977-1981

[2] Kim SJ, Ono T, Esashi M. Mass detection using capacitive resonant silicon resonator employing LC resonant circuit technique. The Review of Scientific Instruments. 2007;**78**:085103

[3] Van Beek JTM, Puers R. A review of MEMS oscillations for frequency reference and timing applications. Journal of Micromechanics and Microengineering. 2012;**22**:013001

[4] Toan NV, Miyashita H, Toda M, Kawai Y, Ono T. Fabrication of an hermetically packaged silicon resonator on LTCC substrate. Microsystem Technologies. 2013;**19**:1165-1175

[5] Toan NV, Toda M, Ono T. An investigation on etching techniques for glass micromachining. Micromachining. 2016;**7**:51

[6] Powell O, Harrison HB. Anisotropic etching of {100} and {110} planes in (100) silicon. Journal of Micromechanics and Microengineering. 2001;**11**:217-220

[7] Sammak A, Azimi S, Izadi N, Hosseinieh BK, Mohajerzadeh S. Deep vertical etching of silicon wafers using a hydrogenation-assisted reactive ion etching. Journal of Microelectromechanical Systems. 2007;**16**:912-918

[8] Hossain KMZ, Patel U, Ahmed I. Development of microspheres for biomedical applications: A review. Progress in Biomaterials. 2015;**4**:1-19

[9] Toan NV, Shimazaki T, Ono T. Single and mechanically coupled capacitive silicon nanomechanical resonator. Micro & Nano Letters. 2016;**11**:591-594

[10] Grosse A, Grewe M, Fouckhardt H. Deep wet etching of fused silica glass for hollow capillary optical leaky waveguides in microfluidic devices. Journal of Micromechanics and Microengineering. 2001;**11**:257-262

[11] Iliescu C, Chen B, Miao J. On the wet etching of pyrex glass. Sensor and Actuators Physics: A. 2008;**143**:154-161

[12] Inomata N, Toda M, Sata M, Ishijima A, Ono T. Pico calorimeter for detection of heat produced in an individual brown fat cell. Applied Physics Letters. 2012;**100**:154104

[13] Inomata N, Toda M, Ono T. Highly sensitive thermometer using a vacuum-packed Si resonator in a microfluidic chip for the thermal measurement of single cell. Lab on a Chip. 2016;**16**:3597

[14] Yamada T, Inomata N, Ono T. Sensitive thermal microsensor with pn junction for heat measurement of a single cell. Japanese Journal of Applied Physics. 2016;**55**:027001

[15] Hanneborg A, Nese M, Ohlckers P. Silicon to silicon anodic bonding with a bonrosilicate glass layer. Journal of Micromechanics and Microengineering. 1991;**1**:139-144

[16] Toan NV, Nha NV, Song Y, Ono T. Fabrication and evaluation of capacitive silicon resonators with piezoresistive heat engines. Sensors and Actuators A. 2017;**262**:99-107

[17] Toan NV, Sangu S, Ono T. Fabrication of deep $SiO_2$ and Tempax glass pillar structures by reactive ion etching for optical modulator. Journal of Microelectromechanical Systems. 2016;**25**:668-674

[18] Toan NV, Sangu S, Ono T. Glass reflow process for microsystem applications. Journal of Micromechanics and Microengineering. 2016;**26**(11):115018 (9 Pages)

[19] Toan NV, Sangu S, Inomata N, Ono T. Glass capillaries based on a glass reflow into nanotrench for controlling light transmission. Microsystem Technologies. 2016;**22**:2835-2840

[20] Mias S, Camon H. A review of active optical devices: I. Amplitude modulation. Journal of Micromechanics and Microengineering. 2008;**18**:083001

[21] Mias S, Camon H. A review of active optical devices: II. Phase modulation. Journal of Micromechanics and Microengineering. 2008;**18**:083002

[22] Toan NV, Sangu S, Saito T, Inomata N, Ono T. Fabrication of a $SiO_2$ optical window for controlling light transmission. Microsystem Technologies. 2017;**23**:919-927

[23] Toan NV, Sangu S, Ono T. Design and fabrication of large area freestanding compressive stress $SiO_2$ optical window. Journal of Micromechanics and Microengineering. 2016;**26**:075016

[24] Nishiyama H, Suga M, Ogura T, Maruyama Y, Koizumi M, Mio K, Kitamura S, Sato C. Atmospheric scanning electron microscope observes cells and tissues in open medium through silicon nitride film. Journal of Structural Biology. 2010;**172**:191-202

[25] Evans JE, Jungjohann KL, Wong PCK, Dutrow GH, Arslan I, Browning ND. Visualizing macromolecular complexes within situ liquid scanning transmission electron microscopy. Micro. 2012;**43**:1085-1090

[26] Hayashi H, Toda M, Ono T. Micro fluidic chamber with thin Si windows for observation of biological samples in vacuum. IEEE international conference on Micro Electro Mechanical Systems. 2015:344-347

[27] Toan NV, Hahng S, Song Y, Ono T. Fabrication of vacuum-sealed capacitive micromachined ultrasonic transducer arrays using glass reflow process. Micromachining. 2016;**7**:76

[28] Tao C, Yin C, He M, Tu S. Thermal analysis and design of a micro-hotplate for silicon substrated micro-structural gas sensor. Proceeding of IEEE-NEMS. 2008:284-287

[29] Partride JG, Field MR, Sadek AZ, Zadeh KK, Plessis JD, Taylor MB, Atanacio A, Prince KE, Mcculloch DG. Fabrication, structural characterization and testing of a nanostructured tin oxide gas sensor. IEEE Sensor Journal. 2009;**9**:563-568

[30] Chen L, Mehregany M. Exploring silicon carbide for thermal infrared radiators. Proceeding of IEEE-Sensors. 2007:620-623

[31] Xu YQ, Wu NJ. Oxide thin film heterostructure IR detector. Proceedings of 17th IEEE-ISAF. 1998:199-202

[32] Mcnab A, Kirk KJ, Cochran A. Ultrasonic transducers for high temperature characterization of micromachined chemical reactions. Proceedings of Tranducers'97. 1997:163-166

[33] Zhang C, Najafi K. Fabrication of thick silicon dioxide layers for thermal isolation. Journal of Micromechanics and Microengineering;**14**:769-774

IntechOpen